Supporting information

Anatase/TiO_2(B) homojunction nanosheets with gold cocatalyst for direct photocatalytic coupling of methane to ethane

Xuanzhao Lu,[b‡] Huanhuan Luo,[b‡] Biyang Xu,[b‡] Zhuo Liu,[b‡] Yue Cao,[a] Kai Li,[c] Xiaohan Yang,[b] Liangyiqun Xie,[b] Tao Guan,[b] Wenlei Zhu,[b*] and Yang Zhou[a*]

[a]*State Key Laboratory for Organic Electronics and Information Displays & Institute of Advanced Materials IAM, Nanjing University of Posts & Telecommunications, Nanjing 210046, China*

[b]*State Key Laboratory of Pollution Control and Resource Reuse, State Key Laboratory of Analytical Chemistry for Life Science, Frontiers Science Center for Critical Earth Material Cycling, School of Chemistry and Chemical Engineering, School of the Environment, Nanjing University, Nanjing 210023, China*

[c]*School of Science, Wuhan University of Science and Technology, Wuhan 430065, China*

Address correspondence to: wenleizhu@nju.edu.cn, iamyangzhou@njupt.edu.cn

‡These authors contributed equally to this work.

Chemicals

Titanium tetrachloride ($TiCl_4$) was purchased from Shanghai Macklin Biochemical Co., Ltd. Methanol, ethylene glycol (EG) and chloroauric acid tetrahydrate ($HAuCl_4 \cdot 4H_2O$) were purchased as A.R. grade from Sinopharm Chemical Reagent Co., Ltd. All of the chemicals were used as received without further purification.

Supplementary Methods

Characterizations.

Powder X-ray diffraction (XRD) patterns were collected on the D8 Advance (Bruker, Germany) with Ni-filtered Cu-Kα (λ = 1.540598 Å). Field emission scanning electron microscopy (SEM, JSM-7800F, JEOL, Japan) and transmission electron microscope (TEM, JEM-2800, JEOL, Japan) were employed for the determination of morphological structure of as-prepared samples, while the elemental mapping of Au-TiO_2 was analyzed by energy dispersive spectroscopy (EDS) attached to the TEM. Elemental compositions were measured by X-ray photoelectron spectrometer (XPS) (PHI5000 VersaProbe, ULVAC-PHI, Japan) using 150 W Al-Kα X-ray sources. Ultraviolet-visible light diffuse reflectance spectrometer (UV-vis DRS) were obtained on a UV-3600 spectrophotometer (Shimadzu, Japan) using ultrafine $BaSO_4$ powder as the reference material. Fluorescence spectrometer (Edinburgh FLS980, Edinburgh, Britain) was used for the collection of PL emission spectra of the samples under 300 nm excitation wavelength. Nuclear Magnetic Resonance (NMR) spectroscopy was conducted on Bruker Advance DRX (400 MHz).

Photoelectrochemical measurements.

Mott-Schottky measurements, transient photocurrent spectra were measured by electrochemical workstation (CHI 660B) using 0.5 M Na_2SO_4 aqueous as electrolyte, with a standard three-electrode system (Pt-counter electrode, Ag/AgCl-reference electrode, sample/ITO-working electrode 1 × 1.5 cm ITO glass plate). The light source for the photocurrent experiments was a 300 W xenon lamp. While electrochemical impedance spectroscopy (EIS) Nyquist plots spectra were tested by identical conditions

but the electrolyte was changed to a mixture of 0.1 M $K_3Fe(CN)_6$, $K_4Fe(CN)_6$, and KCl.

In-situ DRIFTS investigation.

In-situ diffuse reflectance infrared Fourier transform spectroscopy (DRIFTS) measurements were performed using a Bruker TENSOR27 Fourier-transform spectrometer equipped with Harrick diffuse reflectance accessory with ZnSe and quartz window. Each spectrum is recorded by averaging 64 scans at a resolution of 4 cm^{-1}. After sample loading, the pure Ar (99.999 vol%) was purged into the chamber for background spectra collection. Pure CH_4 (99.999 vol%) was then introduced into the chamber and sealed, the CH_4 adsorption spectrum under dark conditions were collected after being undisturbed for 30 min and marked as illuminated sample at 0 min. Then, the system was exposed to light irradiation and the spectra were collected every 3 min.

Catalysts preparation

Synthesis of TiO_2(B) NSs. The TiO_2(B) nanosheets were synthesized by a facile solvothermal method reported by Wang et al.[S1]. Typically, 1 mL $TiCl_4$ was added to 30 mL ethylene glycol at room temperature (25°C) with continuous stirring until no HCl gas was generated. Subsequently, 1 mL of deionized water was added to the suspension, which was stirred for 30 min to form a light-yellow homogeneous solution. The resulting solution was transferred into a 50-mL Teflon-lined stainless-steel autoclave and heated at 150℃ for 4 h. After cooling to room temperature naturally, the white suspension was centrifuged and washed with deionized water and absolute ethanol three times and then dried at 60 ℃ overnight.

Synthesis of Ti300. The synthesis of Ti300 also referenced the method reported by Wang et al.[S1]. The TiO_2(B) NSs were calcined at 300℃ for 4 h in air, with a heating rate of 2℃/min, to remove residual organic matter on the surface and obtain anatase–TiO_2(B) phase homojunctions. This sample was named Ti300. The ratio of anatase/TiO_2(B) or rutile/anatase phases were adjusted using calcination temperatures above 300℃, yielding samples named Ti400, Ti500, etc.

Synthesis of Au_x-Ti300. Referring to the literatures by Long et al.[S2] and Hu et al.[S3], a series of Au_x-Ti samples were synthesized using a modified photo-deposition method, where x represents different Au/TiO_2 weight ratios (wt%). Typically, 0.1 g of as-prepared TiO_2 was ultrasonically dispersed in a mixture of 30 mL of methanol and 15 mL of deionized water. Subsequently, a certain amount of 20-mM aqueous $HAuCl_4$ solution was added to the suspension with continuous stirring. The suspension was placed in a customized photochemical vessel (400 mL in volume) and sealed before being pumped into vacuum. The vessel was irradiated with a 300 W Xe lamp for 30 min with continuous stirring. Finally, the purplish gray suspension was centrifuged and washed with deionized water and absolute ethanol three times and dried at 60℃ overnight.

Photocatalytic activity measurements.

The photocatalytic conversion of methane was performed using a custom flow cell test system. A 300 W Xe lamp (CEL-HXF300, Ceaulight, China) equipped with a UV-Vis reflector (light spectrum range of 320–780 nm) was used as the light source. Typically, 10 mg of catalyst was dispersed in isopropanol (0.5 mL) and drop-coated onto a glass plate (2 × 2 cm). The coated plate was dried in an oven at 60℃ overnight before being placed into a photochemical vessel (30 mL in volume) with a quartz light window on the top. The vessel was purged with 20 mL min^{-1} N_2 gas (≥ 99.999 vol%) for 30 min to remove residual air and then 8 mL min^{-1} CH_4 gas (≥ 99.999 vol%) was continuously flowed through the vessel. Subsequently, a 300 W Xe lamp was turned on to start the photocatalytic methane conversion reaction, with a light power density of 200 mW/cm^{-2}. Circulating water was pumped into the reactor to maintain the catalyst at room temperature. The obtained products were measured every 15 min using a gas chromatograph (GC 8890B, Agilent Technologies, USA) equipped with a thermal conductivity detector (TCD) and a flame ionization detector (FID). The C_2H_6 selectivity in the carbon balance was calculated using the following equation:

$$C_2H_6 \text{ selectivity} = \frac{2n(C_2H_6)}{2n(C_2H_6) + n(CO) + n(CO_2)} \times 100\%$$

NMR spectroscopy measurements.

To verify that the isopropanol from the dispersed catalyst had fully evaporated, we conducted NMR analysis. The procedure was as follows: the dried glass plate was placed in a beaker with 600 μL of water and sonicated for 10 minutes to detach the catalyst from the glass plate and dissolve any residual isopropanol. The resulting suspension was then centrifuged, and 400 μL of the supernatant was mixed with 100 μL of deuterated water containing 25 ppm DMSO as an internal standard for NMR testing. A 1D 1H spectrum was acquired using a water suppression method, with the result shown in Figure S20.

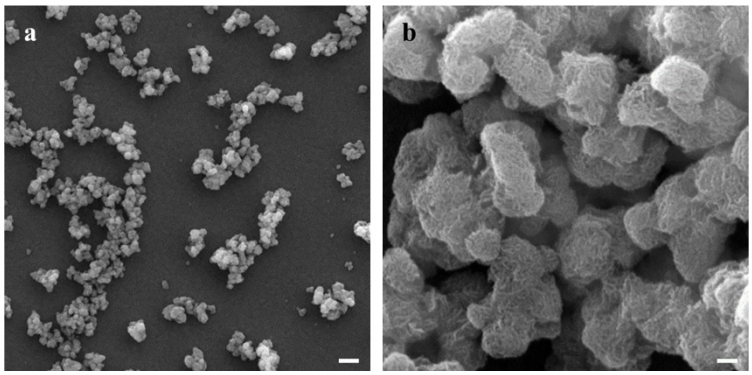

Figure S1. SEM images of TiO_2(B) nanosheets. Scale bar of a (1 μm) and b (100 nm).

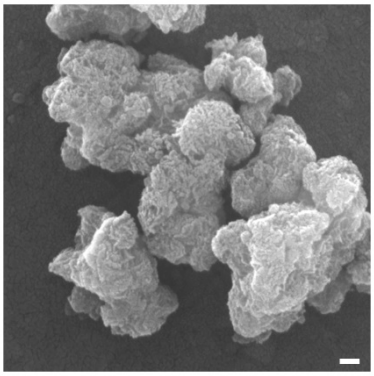

Figure S2. SEM image of $Au_{1.0}$-Ti300 nanosheets. Scale bar, 100 nm.

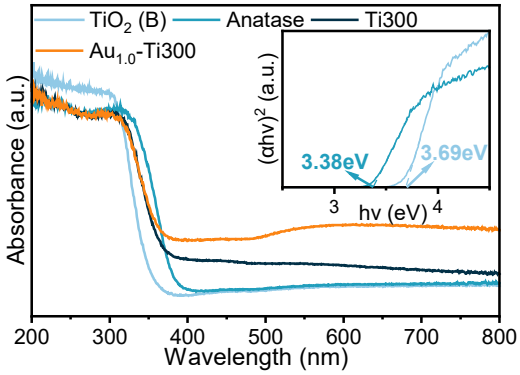

Figure S3. UV-vis DRS of as-prepared samples, with the Tauc plot (inset) for band gap determination using the Kubelka-Munk method. The band gaps were calculated by the equation:

$$\alpha h\nu = A(h\nu - E_g)^{1/2}$$

In which α, h, ν, A, and E_g represent the absorption coefficient, Planck constant, light frequency, proportionality, and bandgap energy, respectively.

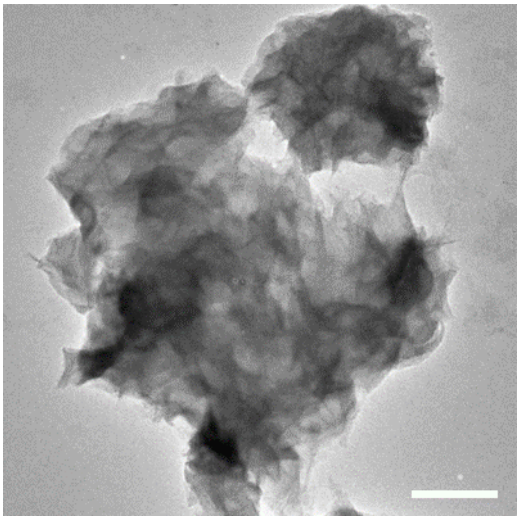

Figure S4. TEM image of TiO_2(B). Scale bar, 100 nm.

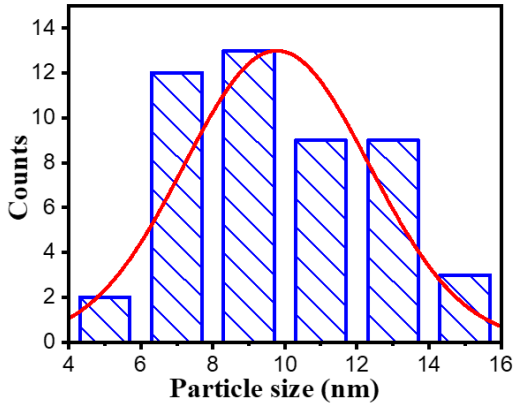

Figure S5. Size distribution of Au NPs on $Au_{1.0}$-Ti300.

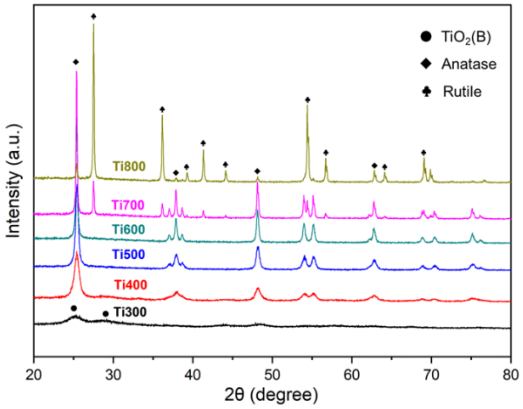

Figure S6. XRD spectra of TiO_2 with different calcination temperatures.

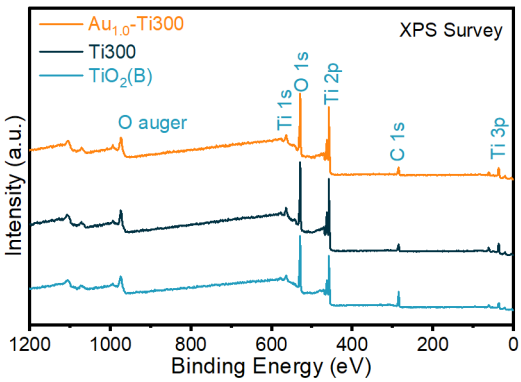

Figure S7. XPS profiles of TiO_2(B) NSs, Ti300, and $Au_{1.0}$-Ti300.

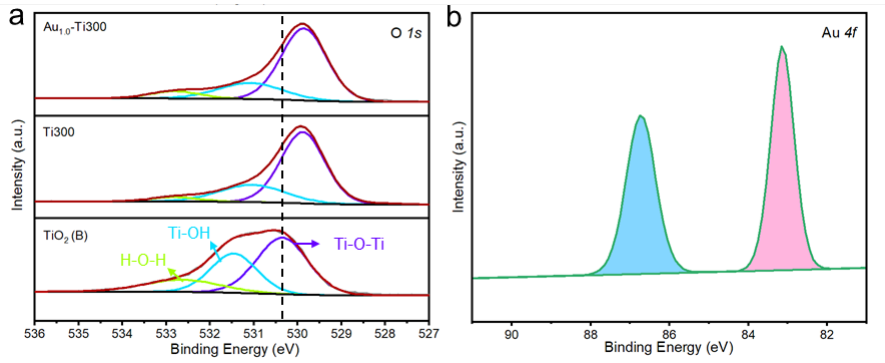

Figure S8. (a) O 1s and (b) Au 4f high-resolution XPS spectra of $Au_{1.0}$-Ti300. The peak in the O 1s region of the TiO_2(B) NSs can be divided into three peaks (530.4, 531.4, and 532.7 eV), indicating the presence of different oxygen species. The peak at 530.4 eV is assigned to the lattice oxygen (Ti–O–Ti) of TiO_2(B), and the peaks at 531.4 and 532.7 eV can be attributed to absorbed hydroxyl groups (Ti–O–H) and water molecules (H–O–H) on the surface of TiO_2(B). The absorbed hydroxyl species (Ti–O–H) correspond to ethylene glycol, which covers the surface of TiO_2(B) to form and stabilize the NS morphology.

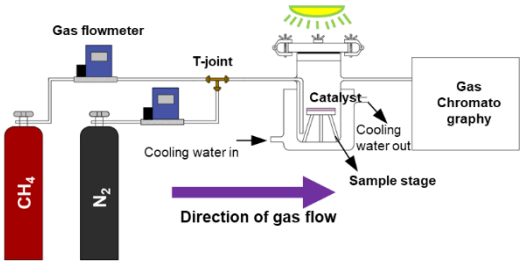

Figure S9. Schematic diagram of the flow-cell photocatalysis system.

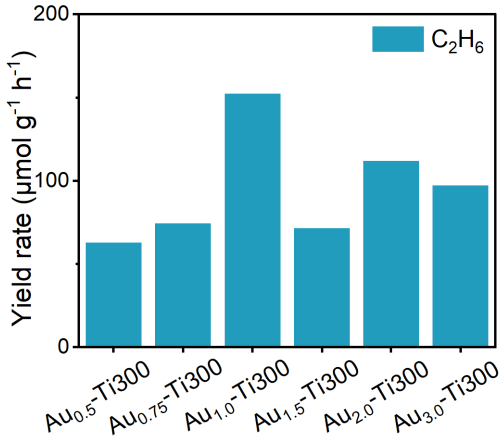

Figure S10. The production rate of C_2H_6 for photocatalytic methane coupling over Au_x-Ti300 with different Au loading amounts.

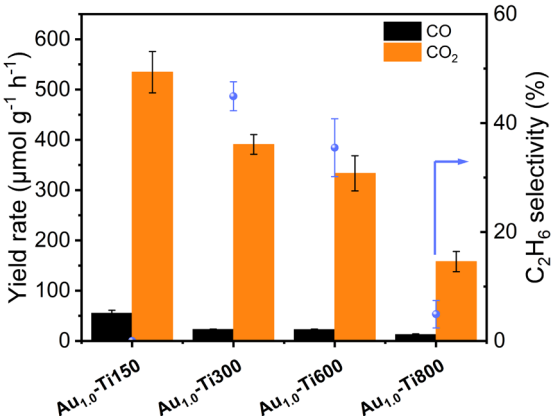

Figure S11. Photocatalytic methane coupling performance (CO and CO_2) over $Au_{1.0}$-Ti with different calcination temperatures.

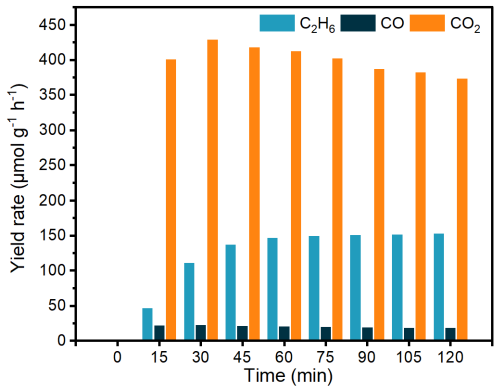

Figure S12. Time course of the photocatalytic product yield rate over $Au_{1.0}$-Ti300. Reaction conditions: 10 mg catalyst, room temperature, 8 mL min^{-1} pure CH_4 flow, atmospheric pressure, 300W Xe lamp (light spectrum 350-780 nm) irradiates for 2 h, light intensity is 200 mW cm^{-2}.

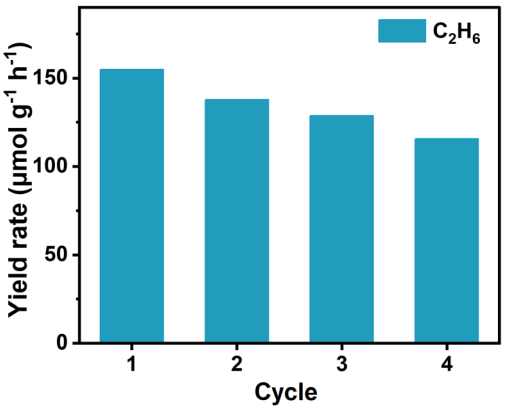

Figure S13. Time course of the photocatalytic C_2H_6 yield rate over $Au_{1.0}$-Ti300.

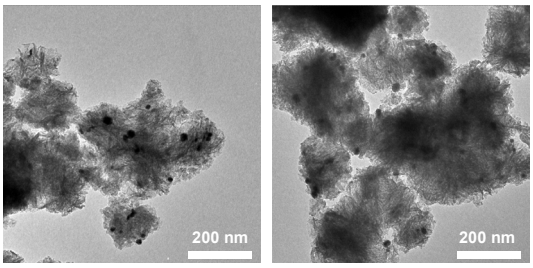

Figure S14. TEM images of $Au_{1.0}$-Ti300 after undergoing four cycles of photocatalytic performance testing.

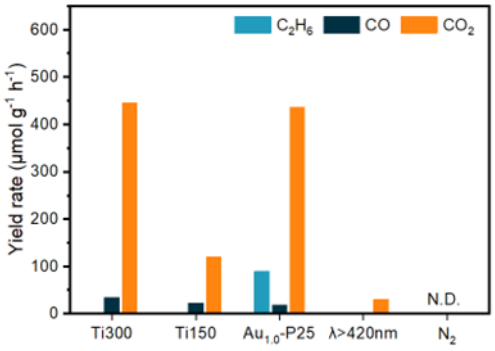

Figure S15. Control experiments of the photocatalytic methane coupling reaction.

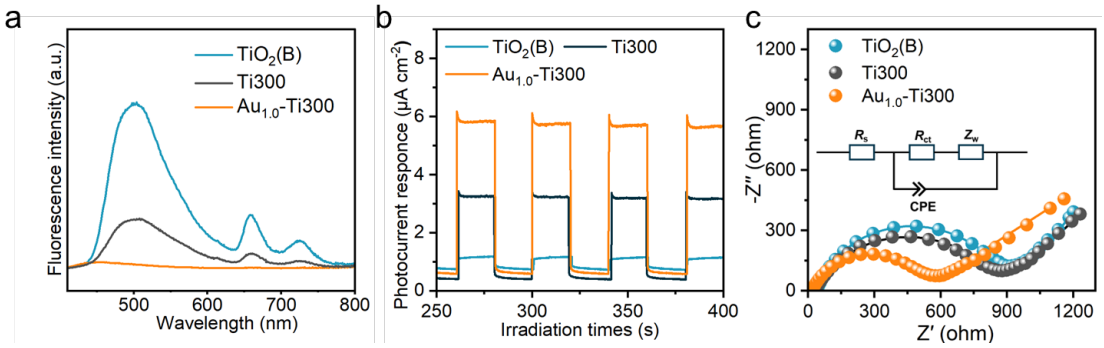

Figure S16. Optical and photoelectrical characterization. (a) Steady-state PL spectra of TiO_2(B), Ti300, and $Au_{1.0}$- Ti300. (b) Transient photocurrent spectra of TiO_2(B), Ti300, and $Au_{1.0}$- Ti300. (c) EIS Nyquist plots and equivalent circuit model of TiO_2(B), Ti300, and $Au_{1.0}$- Ti300. In the equivalent circuit model, *R*s represents solution resistance, *R*ct and CPE are associated with the charge transfer resistance and constant phase element, respectively, and *Z*w is the Warburg impedance related to substance diffusion.

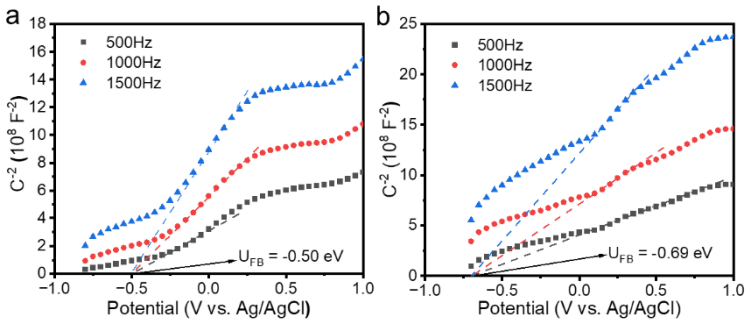

Figure S17. Mott–Schottky plot of (a) TiO_2(B) and (b) anatase TiO_2. The flat band potential is calculated to be −0.30 eV for TiO_2(B) and −0.49 eV for anatase TiO_2 (vs. NHE at PH=7) through the following equation:

$$E(\text{NHE}) = E(\text{Ag/AgCl}) + 0.197$$

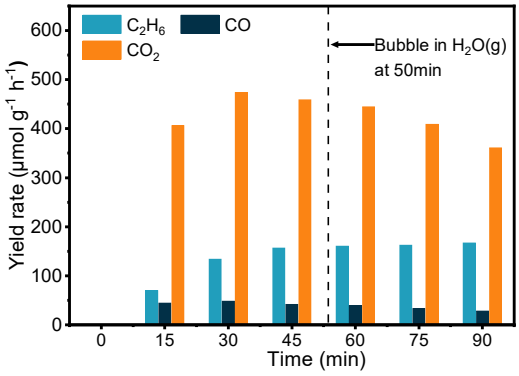

Figure S18. Investigation of the contribution of water to the photocatalytic performance.

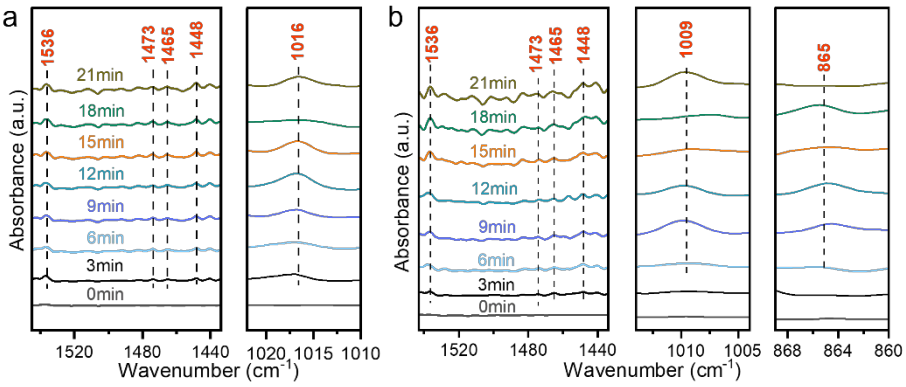

Figure S19. *In-situ* DRIFTS spectra for photocatalytic coupling of CH_4 over (a) Ti300 and (b) $Au_{1.0}$-Ti300.

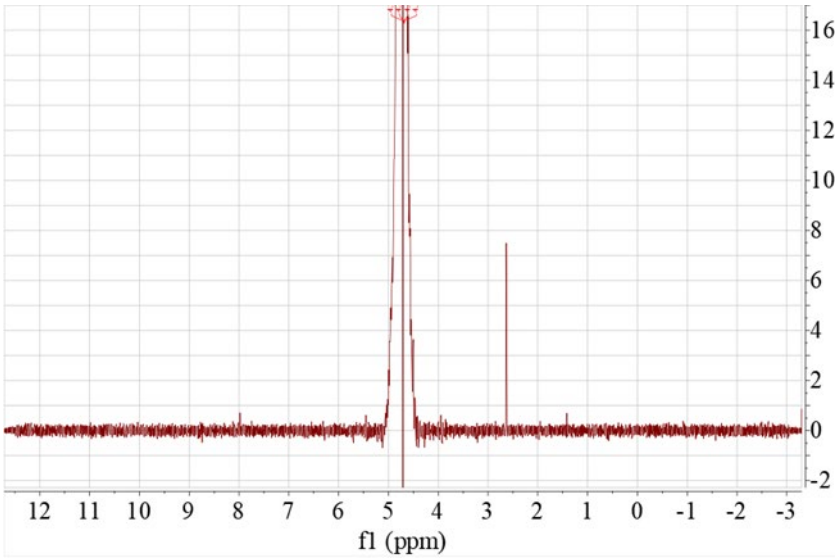

Figure S20. NMR spectrum of supernatant. It can be seen that only the DMSO peak at 2.64 ppm and the water peak at 4.71 ppm are present, with no other peaks. These results indicate that the isopropanol has completely evaporated, having minimal impact on product detection.

Table S1. Quantitative analysis results of Au loading amount on Au_x-Ti300 obtained by ICP-OES.

Catalyst	Au loading (wt%)
$Au_{0.5}$-Ti300	0.64
$Au_{0.75}$-Ti300	0.76
$Au_{1.0}$-Ti300	0.91
$Au_{1.5}$-Ti300	1.12
$Au_{2.0}$-Ti300	1.62
$Au_{3.0}$-Ti300	2.27

Table S2. Representative works in the photocatalytic nonoxidative coupling of methane to ethane using flow reactors.

Photocatalyst	Reaction conditions	Light source	C_2H_6 yield rate (μmol g^{-1} h^{-1})	Ref.
Pd/Ga_2O_3	10% CH_4 in Ar; Flow rate: 30 sccm	Xe lamp 254 ± 10 nm 20mW/cm^{-2}	0.6	S4
$Pd\text{-}Bi/Ga_2O_3$	10% CH_4 in Ar; Flow rate: 30 sccm	Xe lamp (220nm-300nm) 20mW/cm^{-2}	1.4	S5
Au-P25	10% CH_4 in Ar; GHSV: 120000 mL g_c^{-1} h^{-1}	300W Xe lamp with AM 1.5G filter, 100mW/cm^{-2}	81.7	S3
$Au_{1.0}$-Ti300	Pure CH_4, Flow rate: 8 sccm	300W Xe lamp, (350nm-780nm), 200mW/cm^{-2}	170	This work

Table S3. Comparison of equivalent circuit parameters for TiO_2(B), Ti300, and $Au_{1.0}$-Ti300.

Sample	*R*ct (Ω)	*R*s (Ω)
TiO_2(B)	854	38
Ti300	828	30
$Au_{1.0}$-Ti300	509	16

References

S1. G. Xiang, Y.-G. Wang, J. Li, J. Zhuang and X. Wang, *Sci. Rep.*, 2013, **3**, 1411.

S2. L. Meng, Z. Chen, Z. Ma, S. He, Y. Hou, H.-H. Li, R. Yuan, X.-H. Huang, X. Wang, X. Wang and J. Long, *Energy Environ. Sci.*, 2018, **11**, 294-298.

S3. J. Lang, Y. Ma, X. Wu, Y. Jiang and Y. H. Hu, *Green Chem.*, 2020, **22**, 4669-4675.

S4. S. P. Singh, A. Anzai, S. Kawaharasaki, A. Yamamoto and H. Yoshida, *Catal. Today*, 2021, **375**, 264-272.

S5. S. P. Singh, A. Yamamoto, E. Fudo, A. Tanaka, H. Kominami and H. Yoshida, *ACS Catal.*, 2021, **11**, 13768-13781.